Kinetics and Product Studies for Ozonolysis Reactions of Organic Particles Using Aerosol CIMS†

John D. Hearn and Geoffrey D. Smith*

Department of Chemistry, University of Georgia, Athens, Georgia 30602-2556

Received: June 4, 2004; In Final Form: August 6, 2004

The recently developed technique of aerosol chemical ionization mass spectrometry is used to study the reaction of ozone with particles consisting of unsaturated organic molecules, including oleic acid, linoleic acid, oleyl alcohol, and 1-octadecene. The reactive uptake coefficients, γ, for polydisperse aerosols with mean diameters of 800 nm are determined from the rates of loss of the particle species to be $(7.5 \pm 1.2) \times 10^{-4}$ for oleic acid, $(1.1 \pm 0.2) \times 10^{-3}$ for linoleic acid, $(7.5 \pm 1.3) \times 10^{-4}$ for oleyl alcohol, and $(2.4 \pm 0.4) \times 10^{-4}$ for 1-octadecene. The ozonolysis products of oleic acid particles are studied in detail with simultaneous detection of the four primary products: nonanal, nonanoic acid, 9-oxononanoic acid, and azelaic acid. All four products are found to exist in the reacted particles, though nonanal is also detected in the gas phase indicating that it partially evaporates. The yield of azelaic acid is determined to be 0.12 ± 0.04, and the yields of nonanal and 9-oxononanoic acid are found to be larger than the yields of the other products suggesting the existence of secondary reactions involving the Criegee intermediates. A fifth product, 9-oxooctadecanoic acid, is detected with a small yield ($\sim$0.02) and is believed to result from different secondary reactions. Implications of these results for the alteration of chemical and physical properties of aerosols as they are aged in the atmosphere are discussed.

1. Introduction

Aerosols containing organic particles are found throughout the troposphere[1−10] and may significantly affect air quality, visibility, the reflection of solar radiation, the formation of clouds, and human health. The organic component consists of molecules such as alkanes, alkenes, fatty acids, alcohols, and aromatics,[2,11,12] and these species are often found in complex, internally mixed particles. Some of these organics may be surface-active thereby slowing gas transfer into the particles and evaporation of water from them.[13−19] Reactions with trace gas-phase species, such as O_3, OH, HO_2, and NO_3, can transform and age the particles changing the degree of oxidation, altering the particle hygroscopicity and modifying its chemical composition and reactivity.[20,21]

The wide variety of organic species and the many different types of particle morphologies makes it difficult to carefully assess the importance of these transforming reactions. Recent laboratory work has begun to investigate reactions of simple heterogeneous chemical systems that serve as models for more complex particles.[22−38] The reaction of ozone with unsaturated molecules is one such class of reactions being used to validate new experimental approaches and test hypotheses of gas-particle reactivity. In particular, the ozonolysis of oleic acid, an unsaturated carboxylic acid, is emerging as a benchmark reaction used to probe the effects of particle composition and morphology on reactivity. Oleic acid is found in particulate matter in the atmosphere at concentrations of approximately 1 ng/m^3 and is known to originate from a variety of sources, including the broiling of meat.[1,2,39] Additionally, the oleic acid and linoleic acid ozonolysis reactions have been used as models for understanding oxidative damage of lipid membranes.[40]

In this work, we describe the use of the aerosol CIMS (chemical ionization mass spectrometry) technique in studying the ozonolysis of particles consisting of four unsaturated organics: (1) oleic acid, (2) linoleic acid, (3) oleyl alcohol, and (4) 1-octadecene. The gentle ionization afforded by CIMS makes it possible to detect organic species in the particles, as well as in the gas phase, with little fragmentation, thereby simplifying identification and quantification. The uptake coefficients, γ, of these gas-particle reactions are measured by observing changes in particle composition as a function of reaction time in an aerosol flow tube coupled to the aerosol CIMS system. Products are identified from the mass spectra of the reacted particles, and online measurements of both gas-phase and particle species are used to determine the volatility of the products. Additionally, relative product yields from the reaction of O_3 with oleic acid are measured and provide insight into the reaction mechanisms operating in this model gas-particle reaction. Implications of these findings for the application of laboratory particle measurements to atmospheric aerosol reactivity are discussed.

2. Experimental Section

2.1. Particle Generation and Reaction. A log-normal distribution of particles with a mean diameter of 800 nm (geometric standard deviation = $\sigma_g = 1.33$) is generated from the pure organic liquids with a commercial nebulizer (model TR-30-A1, Meinhard, CA). For select experiments in which larger particles are required, homogeneous nucleation of the pure organic liquid is utilized. In this process, particles are created by cooling a saturated vapor of the heated liquid ($T = 80-100$ °C). Particle size distributions are measured with an aerodynamic particle sizer (TSI, model 3321) before and after each kinetics

† Part of the special issue "Tomas Baer Festschrift".

* To whom correspondence should be addressed. Phone: (706) 583-0478. Fax: (706) 542-9454. E-mail: gsmith@chem.uga.edu; www.chem.uga.edu/gsmith.

10.1021/jp0404145 CCC: $27.50
Published on Web 09/30/2004

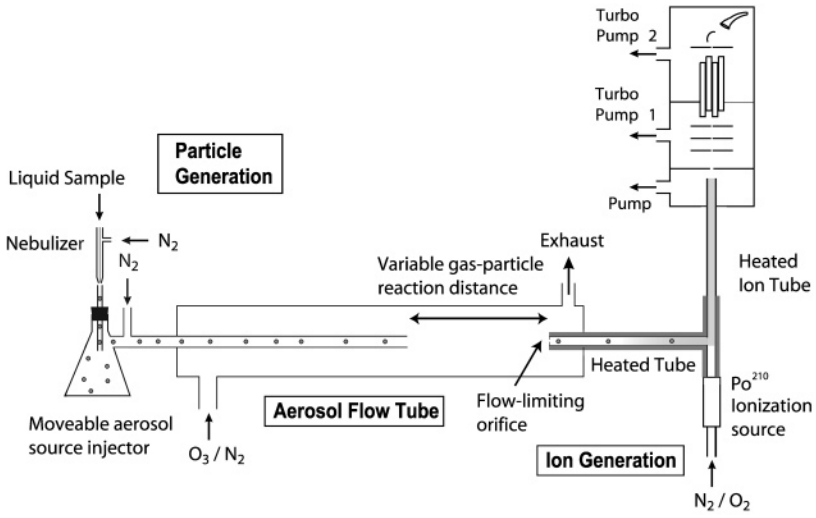

Figure 1. Schematic of the Aerosol CIMS apparatus coupled to the aerosol flow tube. Particles are introduced through a movable injector and then react with O_3 for a variable amount of time before they are sampled through the flow-limiting orifice. The particles are vaporized in the heated tube after which the vapor is ionized and the ions are detected with a quadrupole mass spectrometer. Size distributions of particles exiting the holding flask are measured with an aerodynamic particle sizer (not shown).

experiment and are used in the interpretation of the measured signal decays (see section 2.5). Particles generated with either method are stored in a 500 mL filtration flask containing a stir bar which is used to maintain a uniform particle suspension in the flask. Though the particles settle in the flask, the particle concentration remains sufficiently high to allow experiments to be conducted for at least 1 h. Particles are sampled into the jacketed flow tube through a meter-long, moveable 1/4″ o.d. glass injector (see Figure 1) which allows a variable gas-particle reaction time of up to 4.0 s to be achieved. The particles are entrained in a 4.0 SLPM laminar flow (Re = 200) and remain on-axis for the length of the flow tube. Light from a 532-nm diode laser is scattered by the particles and allows their trajectories in the flow tube to be observed visually. Particle velocities are measured by timing the delay between light scattering events from a particle "packet" at various distances in the flow tube. Measured velocities are typically 23 (±1) cm/s which is within 15% of the calculated laminar flow velocity at the center of the tube.

2.2. Ozone Generation and Measurement. Ozone is generated by flowing approximately 400 sccm of O_2 through a commercial ozone gas generator (model L11, Pacific Ozone Technology, CA) and stored on silica gel (6−12 mesh, Eagle Chemical Co., Mobile, Al) in a glass trap held at −80 °C (in an 2-propanol/dry ice bath). Ozone is sampled into the flow tube by flowing 100 sccm of N_2 through the silica gel and diluting with 0.5 SLPM of N_2. Ozone concentrations are determined with Beer's law in a 10 cm path-length cell with a mercury lamp, a 254 nm (20 nm fwhm) band-pass filter, and a photodiode detector. The ozone flow is further diluted with 3.0 SLPM of N_2 before entering the rear of the flow tube. The O_3 concentration in the flow tube is typically $(2-3) \times 10^{15}$ molecules/cm^3 with an estimated uncertainty of ±10%.

2.3. Chemical Ionization. Particles are sampled through a 500-μm orifice at a measured flow of 2 SLPM and then impact on the walls of the heated vaporizer at a pressure of ∼ 20 Torr. The vaporizer consists of a glass tube (1/2″ o.d., 9 mm i.d., 5″ long) wrapped with Nichrome wire (20 AWG, Arcor, IL) and is typically maintained at ∼350 °C (∼10 ms. residence time for the vapor). The particle vapor is chemically ionized (∼5 ms. reaction time) in the ion tube, a stainless steel tube (1/4″ o.d., 4 mm i.d., 12″ long) wrapped with heating tape and also kept at a temperature of ∼350 °C. Protonated water cluster ions, $H^+(H_2O)_n$, are generated by passing 3.0 SLPM of N_2 and 100 sccm of O_2 through a radioactive static eliminator (^{210}Po, model P-2031, NRD, LLC). Sufficient residual water exists in the system such that $H^+(H_2O)_2$ is the dominant water cluster ion obviating the need to add water vapor. For some of the product identification studies, O_2^- ions are used, and these are selected by simply changing the polarities of the ion optics. The NO^+ ions used in one of the experiments (involving 1-octadecene) are generated by passing 10 sccm of 25% NF_3 in N_2 and 3.0 SLPM N_2 through the polonium ion source.

Ions are drawn into the front chamber by a mechanical pump (Varian DS-400) and then sampled through a 100-μm i.d. orifice into the vacuum chamber which houses the quadrupole mass spectrometer (ABB Extrel, Inc.). This orifice is biased by approximately −30 V (+30 V for negative ions) relative to the ion tube to enhance transmission of the ions, and the ions are further focused by ion optics inside the vacuum chamber. The chamber houses the mass spectrometer and is differentially pumped by two turbomolecular drag pumps (Pfeiffer TMU 520) both of which are backed by a single diaphragm pump (Pfeiffer MVP 055−3). The ions are detected with a Channeltron electron multiplier (Burle) once they are filtered by the quadrupole.

2.4. Chemicals. All chemicals are purchased from Aldrich and used without further purification: oleic acid (90+%, 99+% for uptake experiments), linoleic acid (95%), 1-octadecene (97%), and oleyl alcohol (85%). Gases are purchased from National Welders with the following purities unless otherwise indicated: N_2 (99.99%), O_2 (99.95%), and NF_3 (CP grade).

2.5. Calculation of Uptake Coefficients. Polydisperse particles consisting of the unsaturated liquid of interest (oleic acid, linoleic acid, oleyl alcohol or 1-octadecene) are exposed to O_3 in the aerosol flow tube, and the compositions of these particles are monitored using chemical ionization mass spectrometry. The reactive loss of the species in the particle can be monitored as a function of gas-particle exposure time, and from this observed rate of decay a value of the uptake coefficient can be obtained. This procedure utilizes a standard resistance model which describes many of the processes which determine the rate of uptake of a gas-phase species into a particle and it has been discussed in detail elsewhere.[41−44]

The analysis of O_3 uptake by the particles is the same for all four species used, but to simplify the discussion we will be focusing on oleic acid in particular. As demonstrated previously,[28−30] the reaction of O_3 in oleic acid particles occurs predominantly in a region near the surface (approximately 10−20 nm deep), and the rate of reaction is limited by diffusion of O_3 in the particle. This finding results in a simple analytical solution describing the concentration of oleic acid in the particle as a function of reaction time

$$\sqrt{[\text{oleic}]} = \sqrt{[\text{oleic}]_0} - \frac{3P_{O_3}H\sqrt{Dk_2}}{2a}t \qquad (1.1)$$

where P_{O_3} is the partial pressure of O_3 (in atm), H is the Henry's law solubility constant of O_3 in the particle (in M/atm), D is the diffusion constant of O_3 in oleic acid (in cm^2/s), k_2 is the second-order rate constant for reaction of O_3 with oleic acid (in $M^{-1}\ s^{-1}$), and a is the particle radius (in nm). A reaction occurring only at the surface of the particle or throughout the entire particle would yield a different functional form than eq 1.1,[30,44] though we should point out that we cannot distinguish these three cases using our polydisperse sample. Therefore, we assume that the functional form given in eq 1.1 holds for all of our uptake experiments.

An important consequence of this method of analysis is that the rate of loss of oleic acid is inversely proportional to the particle radius resulting from a dependence on the surface area-to-volume ratio. This dependence is a direct result of the fact that the rate of reaction is proportional to the concentration of O_3 in the particle. The number of O_3 molecules entering the particle is proportional to the surface area ($\sim a^2$), but the concentration of O_3 molecules in the particle is inversely proportional to the volume ($\sim 1/a^3$). However, the uptake coefficient (fraction of gas-particle collisions resulting in reaction) is independent of particle size

$$\gamma = \frac{4HRT}{\bar{c}}\sqrt{Dk_2}\sqrt{[\text{oleic}]} \qquad (1.2)$$

where R is the gas constant (0.082057 L atm/mol/K), T is the temperature (in K), and $\bar{c}$ is the average speed of O_3 in the gas phase (in cm/sec.). Since the parameters H, D, and k_2 appear in both eqs 1.1 and 1.2, a value of γ can be calculated from the measured rate of change of the oleic acid concentration without explicit knowledge of their individual values.

Thus, when a polydisperse particle sample is used, as in these experiments, the uptake coefficient will be the same for all particles, but the observed rate of decay of the particle will be dependent on particle size as in eq 1.1. We have devised a method to obtain a value of γ from such an observed decay by explicitly including the size dependence of the polydisperse particle sample. The distribution of (unreacted) particle sizes is measured both before and after each uptake experiment using the aerodynamic particle sizer. Then, for each size bin, the concentration of the condensed-phase species is calculated as a function of reaction time for an assumed value of γ using eq 1.1. These concentration profiles are then weighted by the particle number density and the average particle volume for each size bin, and a cumulative decay profile of concentration vs reaction time is obtained. This procedure is then repeated for different values of γ until the sum of the squares of the differences between the observed decay data and the predicted curve is minimized indicating the value of γ that best fits the data. For each decay, the values of γ obtained using the two sets of size distribution data (collected before and after the decay) are averaged, and the quoted uncertainty in γ is determined from the difference between these values as well as the estimated uncertainties in $[O_3]$ and the particle velocity.

As this technique used to measure reactive uptake coefficients is unique in many aspects, we feel that it is necessary to address certain points which could possibly present complications in the analysis of the rate data. (1) Particle loss due to settling within the holding flask. The particle signal at the zero-exposure point (injector pushed in completely) is measured both before and after each reactive measurement, thereby allowing us to compensate for particle loss in the flask during the course of the measurement (~2 min). (2) Particle impaction affecting the size distribution measured by the aerodynamic particle sizer. Particles are introduced to the sizer from the holding flask using the same 90° bent tube that is used to introduce them to the moveable injector. Furthermore, size distributions measured at the outlet of the moveable injector appear identical to those taken directly out of the flask. Thus, we conclude that the measured distribution is representative of the particles entering the flow tube. (3) Loss of O_3 on the walls of the injector. The O_3 signal can be monitored as O_3^- with negative chemical ionization and no change in O_3^- signal is detected as the injector is moved within the flow tube. (4) Diffusion of O_3 to the particles may slow reaction at outlet of injector. O_3 is calculated to diffuse from outside of the injector to the middle of the particle stream, a distance of 1/8″, in ~0.4 s. This diffusion effectively reduces the gas-particle reaction time and results in an observed particle decay that is nearly flat at short reaction times (<0.2 s). All particle decays are corrected by subtracting this measured diffusion time of 0.2 s from the calculated reaction times. (5) Incomplete vaporization of the particles. In all of the experiments presented here, the vaporizer and ion-tube temperatures are maintained at ~350 °C, sufficient to vaporize even the least volatile species as demonstrated by a leveling off of the corresponding ion signal.[45] (6) Loss of particles in vaporizer. Particles impacting but not vaporizing would be evident as a persistent background signal in the mass spectrum and this is not observed. Additionally, the fast disappearance (~5 s) of the signal upon removal of the particle source indicates that no particles are condensing within the vaporizer. (7) Vaporized particles react with O_3 in the gas phase. We estimate that once vaporized the particle constituents spend approximately 15 ms in the gas phase during which time they may react with O_3 resulting in additional loss of the particle signal (measured to be ~50%). However, this loss is pseudo-first-order as long as the O_3 concentration is in excess of the concentration of the particle reactant, as is the case for all of our experiments (e.g., $[O_3] = (2-3) \times 10^{15}$ molecules/cm^3, [oleic acid] $= 1-10 \times 10^{11}$ molecules/cm^3). Thus, the fraction of particle vapor which reacts in the vaporizer is the same for all measurements and cancels when normalized to the zero exposure ($t = 0$ s.) measurement.

3. Results

3.1. Uptake by Pure Particles. Values for the uptake coefficients are obtained using the procedure outlined in section 2.5 in which γ is varied to obtain the best fit between the data and the predicted decay curve. Representative decay data for oleic acid particles reacting with O_3 are shown in Figure 2 along with decay curves for various values of γ as calculated with this procedure. The value of γ that best fits the data is 7×10^{-4}. Decay curves for $\gamma = 6 \times 10^{-4}$ and $\gamma = 8 \times 10^{-4}$ systematically underestimate or overestimate, respectively, the rate of decay, thereby demonstrating the precision with which

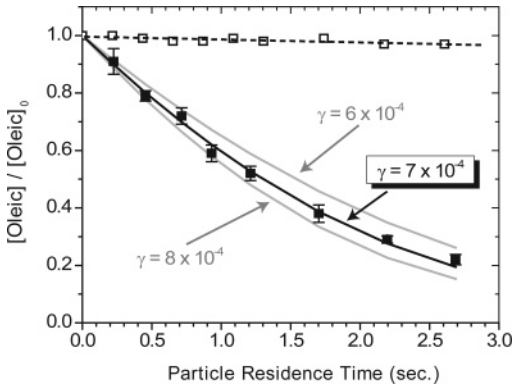

Figure 2. Decay of oleic acid particle signal ($m/z = 283$) as a function of particle residence time in the flow tube: (■) 10^{-4} atm of O_3, (□) no O_3. Lines represent calculated decay curves weighted by particle volume and number density and accounting for size-dependent rate of uptake. The best fit is $\gamma = 7 \times 10^{-4}$. Note that there is only a slight loss of signal in the absence of O_3 indicating that the particles are efficiently transmitted down the flow tube.

TABLE 1: Reactive Uptake Coefficients of O_3 by Particles Containing Unsaturated Organic Species[a]

	γ	σ
oleic acid 800 nm, $\sigma_g = 1.33$	7.5×10^{-4}	1.2×10^{-4}
oleic acid 1.2 μm, $\sigma_g = 1.20$	7.2×10^{-4}	1.1×10^{-4}
oleic acid 1.5 μm, $\sigma_g = 1.34$	7.3×10^{-4}	1.2×10^{-4}
linoleic acid	1.1×10^{-3}	0.2×10^{-3}
oleyl alcohol	7.5×10^{-4}	1.3×10^{-4}
1-octadecene	2.4×10^{-4}	0.4×10^{-4}

[a] σ represents estimated uncertainties in $[O_3]$, the gas-particle reaction time and the particle size distribution. Unless otherwise indicated, the average particle size is 800 nm with a geometric standard deviation of 1.33.

the fitting method can be used. Finally, a decay of oleic acid particles is measured in the absence of O_3 and is also plotted in Figure 2. The nearly constant signal as the particle residence time is varied confirms that the particles are transported efficiently along the axis of the flow tube. The slight decline in the signal allows us to estimate the smallest value of γ that we can measure with this technique as 2×10^{-5}, more than an order of magnitude smaller than the smallest value measured in this work.

We measure the uptake coefficients for four unsaturated organic molecules as shown in Table 1. Unless otherwise indicated, the particles have a mean aerodynamic diameter of 800 nm with a geometric standard deviation of 1.33. The values of γ measured for oleic acid, $(7.5 \pm 1.2) \times 10^{-4}$, and linoleic acid, $(1.1 \pm 0.2) \times 10^{-3}$, compare well with the results of most of the previous studies (shown in Table 2). In particular, the agreement with both coated-wall flow tube studies is very good. Similarly, the coated-wall flow tube study of canola oil (of which oleic acid is a constituent) by DeGouw and Lovejoy[23] indicates a value of $\sim 7.5 \times 10^{-4}$ for the uptake of O_3. Comparison with the only two previous studies to use aerosol mass spectrometers[29,30] to measure uptake kinetics is not as straightforward and is discussed in more detail in section 4.1.

The rates of reaction of O_3 with two other unsaturated organic molecules, oleyl alcohol ($\gamma = 7.5 \times 10^{-4}$) and 1-octadecene ($\gamma = 2.4 \times 10^{-4}$), are also obtained. Oleyl alcohol is detected with proton-transfer ionization using the $H^+(H_2O)_2$ reagent ion, but 1-octadecene is detected through hydride abstraction with NO^+ to eliminate a coincidental product fragment peak that appears at the same nominal mass-to-charge ratio as 1-octadecene, itself. The rate constant, k_2, can be expected to be similar for both oleic acid and oleyl alcohol, but the other parameters which influence the rate of reaction, namely the Henry's law solubility (H) and the diffusion constant of O_3 in the particle (D), may be different for the alcohol than for the acid. However, we find that the uptake coefficients for these two molecules are similar thus indicating that both H and D are either nearly the same for the two molecules or they differ in such a way as to cancel any effect on the rate of uptake. On the other hand, the uptake of O_3 by 1-octadecene is markedly slower than for both oleic acid and oleyl alcohol. This finding suggests that the position of the double bond within the molecule can affect the rate of reaction, as has been pointed out previously.[28,37,46] It should be noted, however, that we cannot rule out the possibility that the decrease in γ for 1-octadecene may in part be due to inhibited solubility or diffusion of O_3 in the particle.

3.2. Uptake by Internally Mixed Particles. We find a larger uptake coefficient for linoleic acid than for oleic acid, consistent with the results of others.[28,37] This increase is thought to be a consequence of the fact that linoleic acid possesses two double bonds whereas oleic acid has only one, effectively making the rate constant for ozonolysis, k_2, twice as large for linoleic acid. Such an increase translates into an expected enhancement of 1.41 in γ according to eq 1.2. Because γ is not just a measure of k_2 but also of H (the solubility) and D (the diffusion) in the particle, it is possible that the ratios of the uptake coefficients may also reflect differences in these parameters for the two species.

To more directly measure the relative rate constants for the two reactions, we measure O_3 uptake by internally mixed particles of oleic acid and linoleic acid. The particles are nebulized from a 1:1 mixture (by mole) of linoleic acid and oleic acid. Uptake coefficients for oleic acid and linoleic acid

TABLE 2: Summary of Experiments Measuring the Reactive Uptake Coefficients of O_3 by Oleic Acid and Linoleic Acid

	this work	Morris et al.[29]	Baer/Miller and co-workers[30]	Moise and Rudich[28]	Thornberry and Abbatt[37]
method	aerosol flow tube	aerosol flow tube	aerosol flow tube	coated wall flow tube	coated wall flow tube
γ (oleic acid)	$(7.5 \pm 1.2) \times 10^{-4}$	$(1.6 \pm 0.2) \times 10^{-3}$	$(1.0-7.3) \times 10^{-3}$	$(8.3 \pm 0.2) \times 10^{-4}$	$(8.0 \pm 1.0) \times 10^{-4}$
γ (linoleic acid)	$(1.1 \pm 0.2) \times 10^{-3}$	N/A	N/A	$(1.2 \pm 0.2) \times 10^{-3}$	$(1.3 \pm 0.1) \times 10^{-3}$
particle size	(0.8−1.5) μm	(0.2−0.6) μm	(1.4−4.9) μm	N/A	N/A
maximum O_3 exposure (atm sec.)	5×10^{-4}	1×10^{-4}	1×10^{-3}	$\sim 10^{-8}$	4×10^{-4}
reactant monitored	oleic acid	oleic acid	oleic acid	O_3	O_3
products identified (oleic acid)	nonanal, nonanoic acid, 9-oxononanoic acid, azelaic acid, 9-oxooctadecanoic acid	none	nonanal (?), 9-oxononanoic acid (?)	nonanal, azelaic acid, hexanoic/ heptanoic acid (?)	nonanal
detection technique	aerosol CIMS	aerosol mass spec.	single-particle mass spec.	gas-phase CIMS	gas-phase CIMS

are determined from the observed rate of loss of the respective ions ($m/z = 283$ for oleic acid, $m/z = 281$ for linoleic acid). In this experiment, the O_3 solubility and diffusion are the same for each reaction, so a difference in the uptake coefficients reflects only a difference in the rate constants. We find that the ratio of uptake coefficients for linoleic acid vs oleic acid is 1.37, slightly smaller than the value of 1.41 predicted from the doubling of k_2. This value is also smaller than the ratio of 1.47 that we measure from pure oleic acid and pure linoleic acid particles, and it may indicate that there is enhanced solubility and/or diffusion of O_3 in the pure linoleic particles. Such a finding would be consistent with the ratios of 1.45 and 1.66 reported by Moise and Rudich[28] and Thornberry and Abbatt,[37] respectively. Further work, including an investigation of how the relative rate constant depends on the concentration of the internally mixed particles, may shed more light on this matter.

In an effort to investigate the role that a residual solvent could have on the uptake of O_3, we also create internally mixed particles from a 3:1 mixture (by volume) of oleic acid and methanol. In these experiments, the particles are continuously generated with the nebulizer to minimize evaporation of the methanol from them in the holding flask. Nevertheless, a large enough concentration of methanol exists in the gas phase that the $H^+(H_2O)_2$ reagent ions are replaced by $H^+(CH_3OH)_2$ ions, but these ions can still be used to detect the oleic acid through proton-transfer ionization. Reactive uptake of O_3 is measured by monitoring the loss of oleic acid in the particle with the procedure outlined above (see section 2.5). To directly evaluate any potential artifacts which may arise from the different ion chemistry, we also conduct separate experiments with pure oleic acid particles using the methanol reagent ion and the water reagent ion. All three experiments are conducted on the same day and under similar conditions (gas flows, O_3 concentration, reaction times). The values of γ obtained for each of these experiments are equal to within 5%, confirming that there is no enhancement in the reactive uptake for particles possessing residual solvent and that experiments employing particles created from solutions in alcohol should be comparable to those using pure particles. It is possible, however, that the presence of methanol may influence the identities and yields of the ozonolysis products.

3.3. Uptake As a Function of Particle Size. As far as we are aware, this work represents the first study in which the composition of a polydisperse sample of particles is used to measure the reaction kinetics of a gas-particle reaction. Therefore, we have developed a new method for interpreting the observed rates of loss of the particle reactants (see section 2.5) which is a function of the distribution of particle sizes. To validate this method of analysis, we measure γ for the ozonolysis of oleic acid using three distinct particle size distributions. With the nebulizer, we create particles which have a mean diameter of 800 nm ($\sigma_g = 1.33$). Through the method of homogeneous nucleation, we create 1.2 μm particles ($\sigma_g = 1.20$) and 1.5 μm particles ($\sigma_g = 1.34$). It is expected that under the conditions employed in this work (i.e., $[O_3] \sim (2-3) \times 10^{15}$ molecules/cm^3, $t = 0-4$ s) γ should be independent of size for all three distributions.[29,42,44,47] Indeed, the uptake coefficients measured are $(7.5 \pm 1.2) \times 10^{-4}$ for 800 nm, $(7.2 \pm 1.1) \times 10^{-4}$ for 1.2 μm, and $(7.3 \pm 1.2) \times 10^{-4}$ for 1.5 μm. Such good agreement confirms that changes in size distributions are accurately accounted for in the procedure that we have developed.

3.4. Ozonolysis Products. Mass spectra of the reacted particles are also used to identify products of the ozonolysis reactions. For example, Figure 3 shows a proton-transfer mass

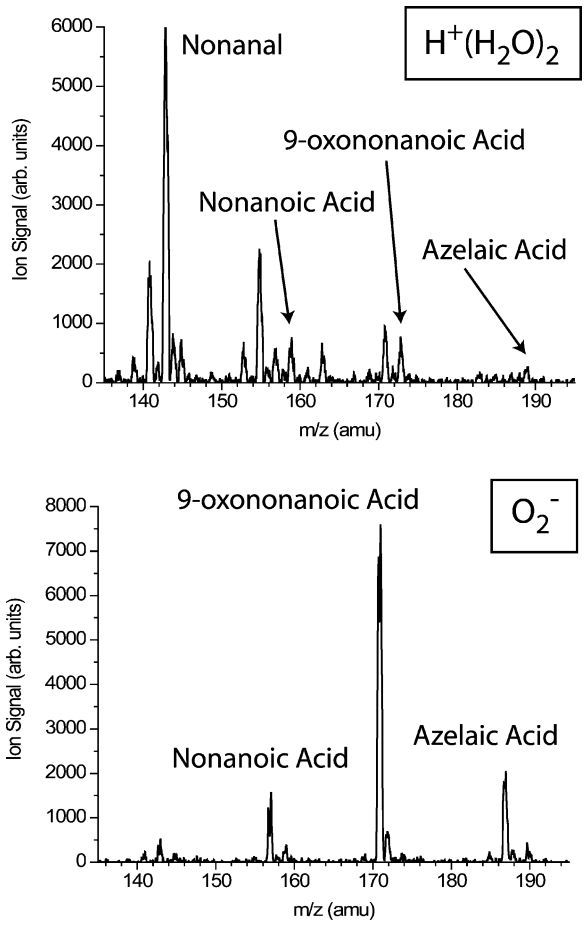

Figure 3. Mass spectra of vaporized oleic acid particles after reaction with O_3. All four expected products, including significant $[M + H - H_2O]^+$ fragment peaks, are identified in the positive proton-transfer spectrum. Only the acidic products are detected in the negative spectrum using the O_2^- reagent ion.

spectrum of vaporized oleic acid particles after reaction with O_3 in the flow tube. There are four products which are expected from this reaction[28-30,37,48] (see Figure 4): nonanal (MW = 142), nonanoic acid (MW = 158), 9-oxononanoic acid (MW = 172), and azelaic acid (MW = 188). Though these products have been observed separately in previous studies,[28-30,36,37] this work and the recent findings of LaFranchi et al.[38] represent the only studies in which they are all observed. A fifth product is also detected at $m/z = 299$ (see Figure 5). We believe that this peak represents 9-oxooctadecanoic acid (MW = 298), a previously unobserved product which results from secondary reactions in the particles.[36] The mechanism for this reaction is discussed in more detail in section 4.2. Further evidence supporting the identification of these products can be seen in the O_2^- spectrum of oleic acid particles reacted offline (Figure 3). In this spectrum, only three of the four expected products, nonanoic acid, 9-oxononanoic acid and azelaic acid, are observed because O_2^- does not abstract a proton from the less acidic nonanal. In addition, a small peak at $m/z = 297$ is also visible (not shown in Figure 3), consistent with the assignment of the $m/z = 299$ peak in the proton-transfer spectrum as 9-oxooctadecanoic acid.

Proton-transfer spectra of the other reacted particles, consisting of linoleic acid, oleyl alcohol, and 1-octadecene, are shown in Figure 6. These ozonolysis reactions are expected to proceed through mechanisms similar to that for oleic acid, and in fact, many of the analogous products are identified. Linoleic acid, however, is an exception since its two double-bonds provide

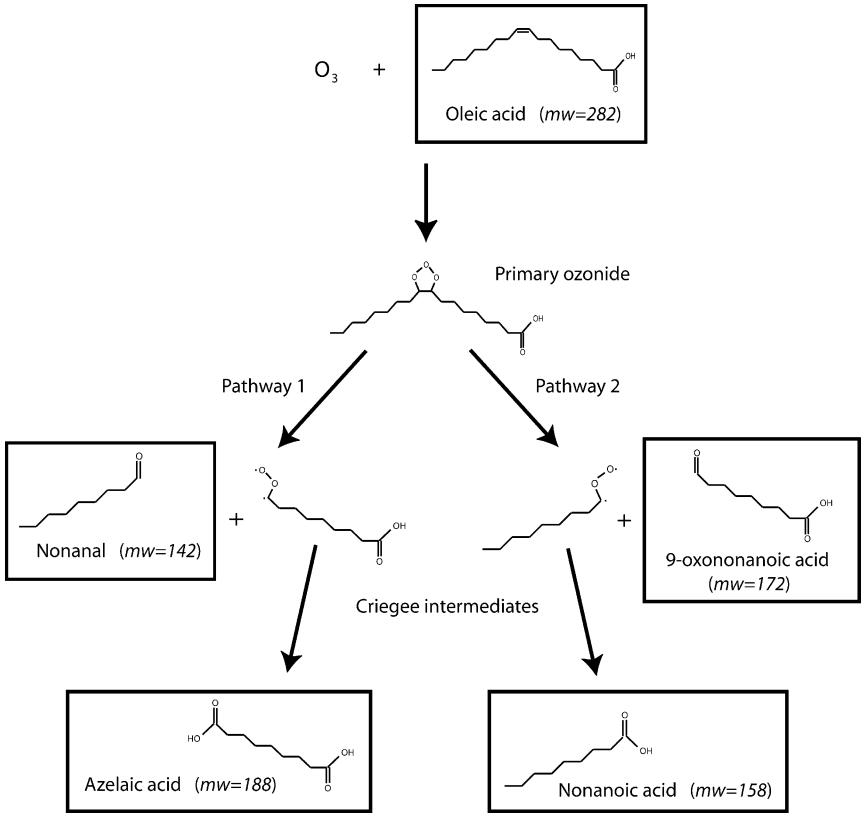

Figure 4. Mechanism of oleic acid ozonolysis showing two pathways for bond cleavage. The Criegee intermediates can rearrange to form the corresponding carboxylic acid products, azelaic acid or nonanoic acid. This mechanism predicts equal yields of 0.5 (moles of product per mole of oleic acid reacted) for each product.

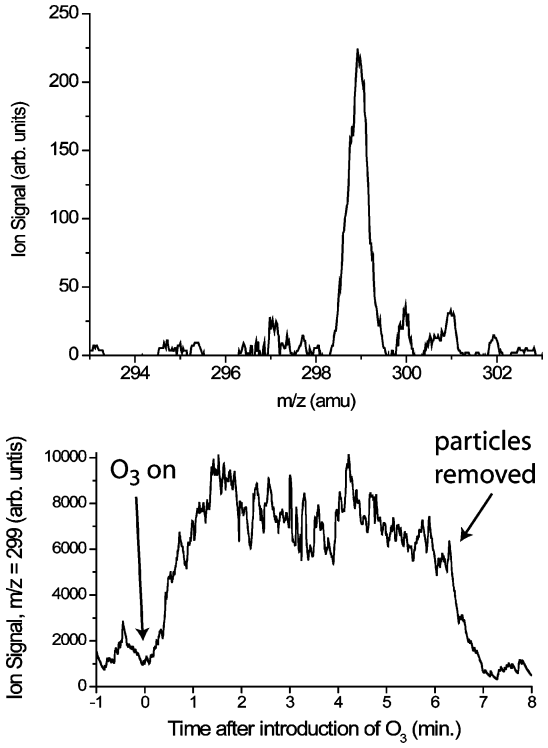

Figure 5. Proton-transfer spectrum of the fifth product from oleic acid ozonolysis, believed to be 9-oxooctadecanoic acid (MW = 298). The trace shows the appearance of the $m/z = 299$ signal when the O_3 is introduced and its disappearance when the particles are directed off-axis, indicating that the product associated with this peak resides on the particles.

two separate sites at which the O_3 can react. Consequently, there are eight possible primary products, seven of which can be found in the positive ion spectrum displayed in Figure 6: hexanal, hexanoic acid, nonenal, nonenoic acid, 9-oxononanoic acid, azelaic acid, and 9-oxododecenoic acid. Several of these products have been observed previously by other researchers.[28,37] Ozonolysis of oleyl alcohol particles yields nonanal, nonanoic acid, 9-hydroxynonanoic acid, and 9-hydroxynonanal, whereas reaction of the terminal alkene, 1-octadecene, results in the formation of formaldehyde, formic acid, heptadecanal, and heptadecanoic acid.

3.5. Product Volatility. The ability to concurrently detect species both in the gas phase and in the particles makes it possible to use aerosol CIMS to determine which of the reaction products remain on the particle and which evaporate from it. In these experiments, the particles are reacted off-line in the holding flask and then are transported through the flow tube either on-axis (down the center) or off-axis (toward the wall) by simply changing the angle of the injector. Consequently, the off-axis particles are not sampled into the vaporizer, as confirmed both by observations of the particle trajectories and the lack of signal from nonvolatile particle species in the mass spectrum. Thus, only gas-phase species contribute to the observed off-axis mass spectrum, and a difference between the on-axis and off-axis spectra indicates the extent of evaporation from the particle.

For example, the integrated signals for the nonanal ($m/z = 143$) and the nonanoic acid ($m/z = 159$) products of oleic acid ozonolysis are shown in Figure 7. When the particles are directed off axis, the nonanoic acid signal drops to its baseline level, whereas the nonanal signal only drops by a fraction. This difference indicates that the nonanoic acid product resides almost entirely on the particle but that the nonanal product is volatile and partially evaporates from the particle. In fact, nonanal is the only volatile product that we observe from this reaction,

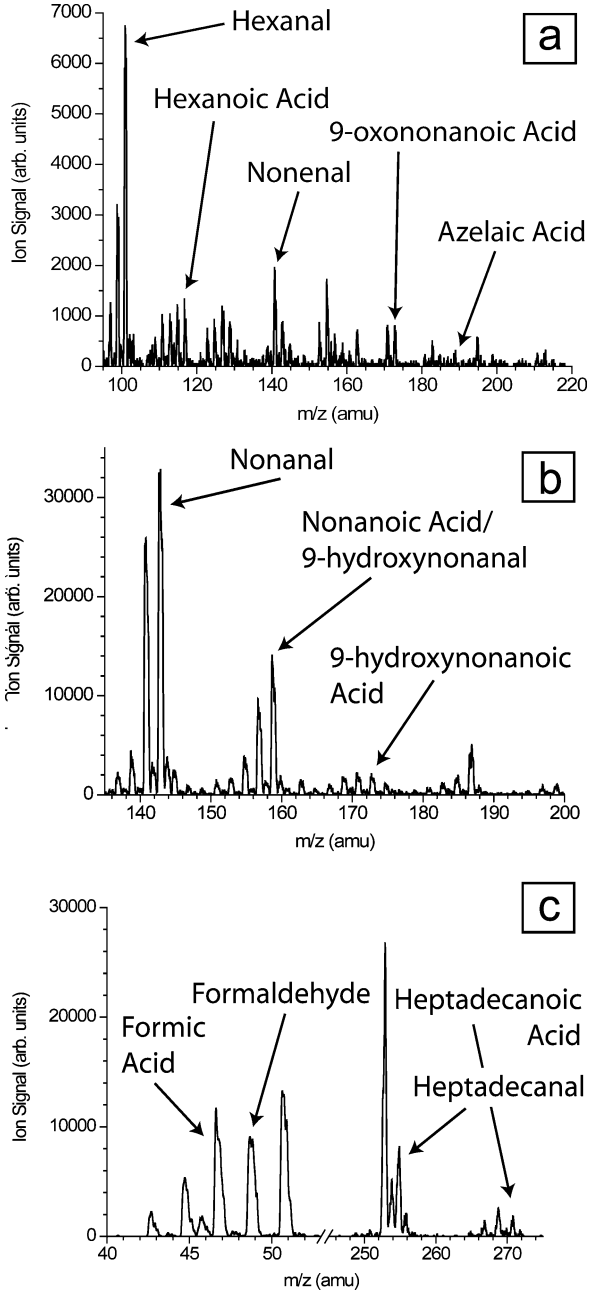

Figure 6. Proton-transfer mass spectra of vaporized particles after reaction with O_3: (a) linoleic acid. In addition to the products identified, nonenoic acid ($m/z = 157$) and 9-oxododecenoic acid ($m/z = 213$) are observed. (b) oleyl alcohol. (c) 1-octadecene. Note that formaldehyde is detected as a water cluster ion, i.e., $[M + H]^+(H_2O)$, $m/z = 49$.

consistent with the findings of Moise and Rudich[28] and Thornberry and Abbatt.[37] Interestingly, the nonanal signal displays a slight jump (dip) when the injector is placed on (off) axis, presumably due to the fact that gas-phase nonanal travels faster in the center (on axis) of the laminar flow than near the walls (off axis). Thus, when the injector is reoriented on axis, there is a temporary increase in the nonanal signal as the faster, on-axis nonanal "catches up" with the slower, off-axis nonanal. We do not observe these jumps or dips with any of the other oleic acid products. The volatile products found from the ozonolysis of the other particles are hexanal, hexanoic acid, nonenal and nonenoic acid for linoleic acid, nonanal for oleyl alcohol, and formaldehyde for 1-octadecene.

It is not possible to calculate exactly how much of the nonanal remains on the particle since the gas-phase nonanal concentration may be artificially increased by evaporation from reacted particles lost on the walls of the flask or by ozonolysis of oleic acid deposited on the walls. Nonetheless, the substantial drop in signal when the particles are directed off-axis indicates that a sizable fraction of the nonanal remains on the particles over the time scale of our experiments (i.e., minutes), consistent with the recent findings of LaFranchi et al.,[38] who detected a small nonanal signal from reacted particles even after they were sampled into a vacuum chamber. We believe that such observations may indicate that other products, namely azelaic acid and 9-oxononanoic acid, reduce nonanal's effective vapor pressure. Such a reduction in volatility could serve to trap some species in organic particles as they age in the atmosphere with potentially significant impacts on their chemical and physical properties. Additional experiments, such as those employing internally mixed particles, are warranted to determine the magnitude of any such volatility effect on particle transformation or activation.

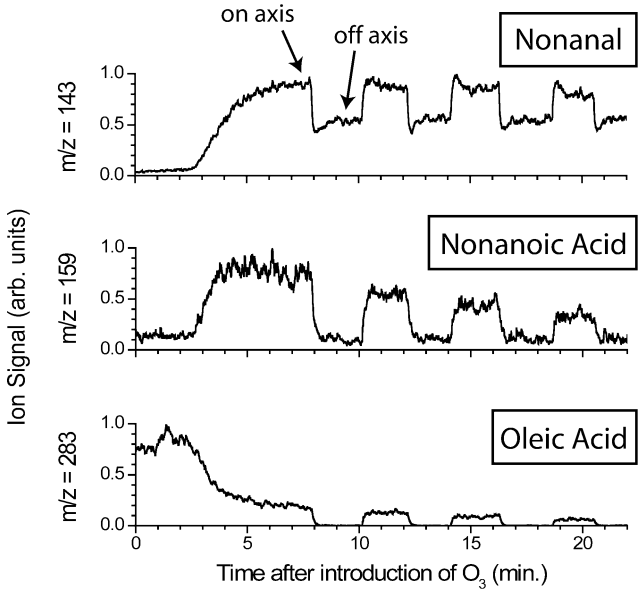

Figure 7. Ion signals for oleic acid and two of the ozonolysis products demonstrating the ability to sample only gas-phase species when the particles are directed off axis. Nonanoic acid remains on the particle but nonanal evaporates incompletely.

It might appear to be more desirable to carry out the reaction in the flow tube so that the exposure time and O_3 concentration can be controlled. However, such an online reaction would be much more complicated to interpret since the reaction time in the flow tube changes when the particles are directed off-axis. Additionally, we believe that any variations in O_3 exposure in our experiments are negligible since we find similar results with repeated offline measurements. Finally, it is conceivable that the observed change in nonanal signal could result from the loss of nonanal vapor in the flow tube when the particle flow is directed off-axis. However, no such change is observed when pure nonanal vapor is flowed through the injector and then detected both on-axis and off-axis. Thus, we conclude that the change in the nonanal signal results from incomplete evaporation from the reacted particles.

3.6. Product Yields for O_3 + Oleic Acid. The addition of O_3 across the double bond is believed to form a primary ozonide which dissociates along two different pathways depending on which O−O bond is broken.[49] Each pathway results in the formation of an aldehyde/ketone and an excited Criegee intermediate (or Criegee biradical)[48] (shown in Figure 4). These excited Criegee intermediates can then decompose, form

stabilized Criegee intermediates (SCI), or rearrange to carboxylic acids. In the absence of additional reactions or dissociation of the SCI, the primary product pairs which are formed from the ozonolysis of oleic acid are as follows: (1) nonanal and azelaic acid and (2) nonanoic acid and 9-oxononanoic acid. It is believed that there will be no preference regarding which of the O−O bonds breaks simply because the carboxylic acid functionality of oleic acid is sufficiently removed from the double bond.[46] Thus, a yield of 0.5 (moles of product per mole of oleic acid reacted) would be expected for each product assuming complete rearrangement of the SCI to form the carboxylic acid products. If, on the other hand, the SCI undergo further reactions with the primary products to form secondary ozonides or with other SCI to form the aldehydic primary products (nonanal and 9-oxononanoic acid), the distribution of the product yields may be altered. The existence of such secondary reactions is supported by our yield observations, namely that (1) the product yields within each pathway are not equal and (2) the azelaic acid yield is less than 0.5. These secondary reactions are discussed in more detail in section 4.2.

The yield measurements are made by reacting oleic acid particles in the flow tube to near completion (i.e., less than 5% of the initial oleic acid signal remains), thus ensuring that the gas-phase reaction in the vaporizer does not contribute significantly to the depletion of oleic acid or to the product signals. Since some of the reaction products may be volatile, we reduce the total flow through the flow tube (2.2 SLPM) to more closely match the sampling rate into the mass spectrometer (2 SLPM), thus ensuring that nearly all of the gas phase is sampled. With the smaller flow, we find that it is necessary to fill the jacket of the flow tube with water to minimize the thermal gradient near the inlet and maintain the particle sampling efficiency.

It is not possible to make direct measurements of the yields for all of the products because it is difficult to determine the absolute detection sensitivities for each species. The wide range of vapor pressures from nonanal (∼300 mTorr at 22 °C[37,50,51]) to nonanoic acid (∼1 mTorr at 20 °C[50]) to azelaic acid (∼4×10^{-6} Torr at 20 °C[13]) makes even relative measurements difficult. Even so, the yield of azelaic acid can be determined by measuring its detection efficiency relative to oleic acid using internally mixed particles. A known amount of azelaic acid is heated (∼80 °C) with a known amount of oleic acid until the two species are well mixed, and then the warm liquid is nebulized to create internally mixed particles. By comparing the corresponding ion signals ($m/z = 189$ for azelaic acid, $m/z = 283$ for oleic acid), we determine the relative detection efficiency of azelaic acid to be 1.3 (±0.4). Using this sensitivity, we calculate the azelaic acid yield from the ozonolysis of oleic acid to be 0.12 (±0.04). In the only other study to measure this yield, Martin and co-workers report values ranging from 0.02 to 0.06.[36] Both studies' yields are much lower than the value of 0.5 that would be predicted from a simple dissociation of the primary ozonide in the absence of any secondary reactions, and in section 4.2, we discuss possible reasons for this discrepancy.

We can also qualitatively compare the yields within each pathway by making a few simple assumptions about detection sensitivities. For pathway 1, we assume that the products, nonanal and azelaic acid, are detected with equal efficiency using the $H^+(H_2O)_2$ reagent ion (Figure 3). The ratio of the nonanal signal ($m/z = 143$) to the sum of the azelaic acid signals ($[M + H]^+$ at $m/z = 189$ and $[M + H - H_2O]^+$ at $m/z = 171$) is measured to be ∼7, implying that the nonanal yield is also seven times larger than that of azelaic acid. Thus, we tentatively estimate the nonanal yield as 0.84, consistent with the requirement that the sum of the yields of the products in each channel equals 1 (in the absence of other reaction pathways). We need to caution, however, that this estimate is based on a rather general assumption of relative detection sensitivities. Additionally, this estimate probably represents a lower bound on the ratio because the detection sensitivity to azelaic acid may be higher if the additional carboxyl group stabilizes the ion. In fact, we see evidence of such stabilization in a 4-fold enhancement in sensitivity to azelaic acid (sum of $m/z = 171$ and $m/z = 189$) compared to oleic acid ($m/z = 283$).

For pathway 2, we use the negative ion spectrum (Figure 3) to compare the yield of 9-oxononanoic acid ($m/z = 171$) to that of nonanoic acid ($m/z = 157$). This spectrum represents oleic acid particles reacted with O_3 offline in the holding flask and then analyzed using the O_2^- reagent ion. Online reactions are not possible using this ion since O_3 depletes it, thereby making it difficult to directly compare this spectrum to the online positive ion spectrum. Nevertheless, the simplicity of this spectrum allows us to reasonably assign equal detection sensitivities to nonanoic acid and 9-oxononanoic acid by assuming that O_2^- abstracts the acidic proton from each with little stabilization contributed by the additional carbonyl of 9-oxononanoic acid. Consequently, we find that the 9-oxononanoic acid yield is five times as large as that of nonanoic acid. If we assume that the yields for these two products sum to 1, we can tentatively assign values of 5/6 (∼0.83) and 1/6 (∼0.17) to 9-oxononanoic acid and nonanoic acid, respectively. As with the estimated nonanal yield, caution should be employed when using these values since they are based on rather broad assumptions. Nonetheless, we can state that the two products that result from the rearrangement of the Criegee intermediates, nonanoic acid and azelaic acid, are found with yields that are substantially less than the yields of their counterparts. In section 4.2 we discuss the implications of these findings for understanding the reaction mechanisms in the particles.

4. Discussion

4.1. Kinetics of Ozonolysis. The values of γ measured for oleic acid and linoleic acid in the current study agree well with the two coated-wall flow tube studies of Moise and Rudich[28] and Thornberry and Abbatt[37] (see Table 2). This level of agreement indicates that the method of analysis accurately accounts for the range of particle sizes in our experiment. In addition, it also suggests that there is no significant systematic difference between the different approaches, namely observing organic particles as they react with O_3 vs monitoring O_3 loss on a coated flow tube. Finally, in our aerosol study, the compositions of the particles are altered drastically as they often react to near completion, whereas the thick (∼1 mm) organic films used in the coated-wall studies[28,37] remain essentially unchanged. The agreement between our particle study and the coated-wall studies leads us to conclude that the substantial transformation of the particles does not influence the rate of reactive uptake.

The O_3 uptake coefficients of oleic acid measured using aerosol mass spectrometers differ substantially.[29,30] Morris et al. measured a value of $\gamma = 1.6 \times 10^{-3}$ independent of particle size for particles 200, 400, and 600 nm in diameter,[29] whereas Baer and co-workers report values of γ ranging from 1.0×10^{-3} for 4.90 μm particles to 7.3×10^{-3} for 1.36 μm particles.[30] In the current study, we find that the uptake coefficient is 7.5×10^{-4} independent of particle size (for average diameters of 800 nm, 1.2 μm, and 1.5 μm). From these three studies, we

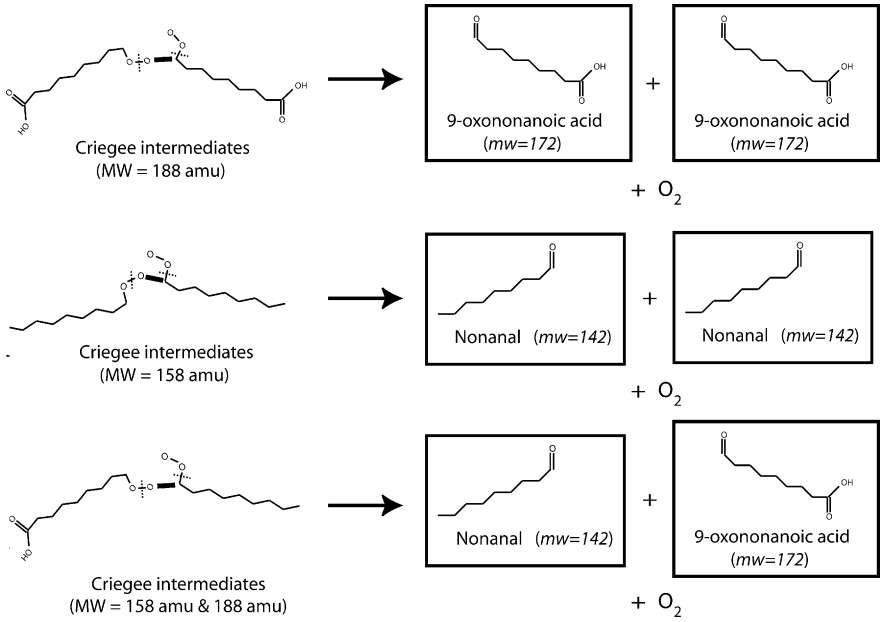

Figure 8. Mechanism by which Criegee intermediates react with each other to form two of the primary ozonolysis products. This mechanism is proposed to explain the larger yields of nonanal (relative to azelaic acid) and 9-oxononanoic acid (relative to nonanoic acid) observed in the ozonolysis of oleic acid.

suggest that the findings of Baer and co-workers may have resulted from an artifact of their technique, namely that the use of a CO_2 laser to vaporize the particles prior to analysis might have artificially increased the observed rate of decay due to greater heating of the particle as it was oxidized. Such an effect would be consistent with the higher values of γ reported in that study. Likewise, the faster rate of oleic acid disappearance measured by Morris et al. using flash vaporization may have resulted from increased fragmentation or incomplete vaporization of the particles. The current study would not be subject to such heating artifacts since the particles are thermally vaporized. In addition, Morris et al. included a longer O_3 diffusion time to the particles than we use (0.35 vs 0.2 s), and this will result in a faster observed rate of oleic acid decay.

We conclude from the results of our experiments and those of Moise and Rudich,[28] Morris et al.,[29] and Thornberry and Abbatt[37] that the reactive uptake coefficient for O_3 by oleic acid is on the order of 10^{-3}. Thus, approximately one in 1000 collisions results in reactive loss of oleic acid, whereas analogous reactions of O_3 with alkenes in the gas phase typically proceed with rate constants of $10^{-15}-10^{-17}$ cm^3/molecule/s,[12] equivalent to approximately one reaction per 10^5-10^7 collisions. Such an enhancement in the reaction rate has been pointed out before,[25,29,37,52] but it is still an open question as to what causes it and to what extent it affects the processing of atmospheric particles. Recent molecular dynamics simulations by Tobias and co-workers[53] indicate that the O_3 lifetime is increased by uptake into the interior of the organic phase, and this could explain the experimentally observed enhancement in the rate of reaction.

Applying the value of $\gamma = 10^{-3}$ to a polluted atmosphere with 100 ppb of O_3, we predict an oleic acid lifetime (in particles) of a few minutes, in sharp contrast to the estimated lifetime of days implied by field measurements as previously indicated.[29,37] This discrepancy may be attributable to factors important only for atmospheric particles, such as morphology or the presence of other particulate constituents.[29,30,54] At this time, we recommend that caution be employed when applying the results of laboratory measurements to atmospheric particles until the roles of these and other such factors are explored further.

4.2. Secondary Reactions Involving Criegee Intermediates. The stabilized Criegee intermediates (SCI) may react with the primary ozonolysis products to form secondary ozonides or with carboxylic acid solvents to create peroxides. Such products have been observed by Rebrovic for the ozonolysis of oleic acid using ^{1}H NMR,[55] though yields were not reported. Each of these reactions represents a loss of the SCI and would be consistent with our observation of enhanced product yields for nonanal and 9-oxononanoic acid relative to nonanoic acid and azelaic acid. However, no evidence for the formation of the secondary ozonide or the peroxides is found in the current study, though it is possible that these species decompose when the particles are vaporized. Additional work will be required to determine whether such species can be detected with the aerosol CIMS technique.

It is also possible that the Criegee intermediates may react with one another to form the aldehydic primary products, nonanal and 9-oxononanoic acid (see Figure 8). Such secondary reactions are believed to explain anomalously large aldehyde yields observed in previous olefin ozonolysis studies.[48,56,57] Indeed, we find that the nonanal yield is substantially larger than the azelaic acid yield and that the 9-oxononanoic acid yield is substantially larger than the nonanoic acid yield (see section 3.6). We believe that the apparent discrepancy between this result and the 0.50 nonanal yield reported by Thornberry & Abbatt[37] can be explained by the much higher concentration of O_3 used in our particle experiments (10^{-4} atm) compared to their coated-wall flow tube experiments (3×10^{-7} atm). The higher O_3 concentration reacts away a significant fraction of each particle, whereas the lower O_3 concentration does not substantially alter the composition of the thick ($\sim$1 mm) oleic acid films. Consequently, the concentration of Criegee intermediates is expected to be much higher in the particles than in the films thereby increasing the rates of the Criegee self-reactions and increasing the nonanal and 9-oxononanoic acid yields.

The proposed mechanism may also explain the interesting trends in product yields observed by Martin and co-workers for the reaction of O_3 with particles coated with oleic acid.[36] In that work, they report an increase in the yield of 9-oxononanoic

acid as the coating thickness was varied from 2 to 30 nm, and they interpret this as evidence for a transition between surface and bulk reactions. However, they reacted each coating to the same extent (reacting away 95% of each coating) by increasing the O_3 concentration from 1 to 30 ppmV ($\sim 2.5-75 \times 10^{13}$ molecules/cm^3) as the thickness was increased. Thus, the thicker coatings may have had a higher concentration of Criegee intermediates near the surface resulting from the higher O_3 concentrations, and the rates of the self-reactions and ultimately the concentrations of 9-oxononanoic acid and nonanal may have been enhanced. It is not clear if this mechanism was indeed operative in the coated particle experiments, but measurements of uptake kinetics performed as a function of coating thickness may offer more insight into this possibility.

Concentrations of O_3 in the troposphere are much lower than those used in our experiments, with typical concentrations ranging from 10 ppb to as high as 500 ppb in the most polluted environments.[12] As such, the concentrations of Criegee intermediates in most organic particles are not expected to be large enough for the proposed mechanism to be of significance. However, these reactions may be operative for certain particle morphologies. For example, a very viscous particle may trap O_3 molecules near the surface, creating a high concentration of Criegee intermediates in this region. Alternatively, high surface area-to-volume ratios, such as in particles with thin coatings of organics, may serve to increase the concentration of Criegee intermediates. Additional work with different types of particles and morphologies should shed some light on the importance of these reactions in the atmosphere.

In addition to the four primary products, we also observe a small peak at $m/z = 299$ in the proton-transfer spectrum and one at $m/z = 297$ in the O_2^- spectrum, suggesting a molecule with a molecular weight of 298 amu. Interestingly, these observations correspond to a secondary product predicted by a mechanism recently proposed by Martin and co-workers.[36] In this mechanism, a Criegee intermediate adds across the double bond of a second oleic acid molecule to form a C_{27} product which can dissociate to 9-oxooctadecanoic acid (MW = 298) and one of the primary ozonolysis products, either 9-oxononanoic acid or nonanal. Such a reaction could affect measured rates of oleic acid loss (as in this work) since it would remove a second oleic acid molecule. However, we estimate that the yield for 9-oxooctadecanoic acid is approximately 0.02, assuming that its detection efficiency is similar to that of oleic acid. We believe that this value is an upper bound on the yield since the additional carbonyl in the 9-oxooctadecanoic acid product may stabilize the ion relative to the oleic acid ion. Consequently, we conclude that this reaction does not represent an important loss of oleic acid in our experiments.

Though Martin and co-workers do not identify this secondary product in their spectra, they do see an enhanced yield of the 9-oxononanoic acid product (MW = 172), consistent with their mechanism. Likewise, Baer and co-workers report a large feature at $m/z = 155$ which they attribute to a fragment of 9-oxononanoic acid.[30] However, since either Criegee intermediate could add across the double bond of oleic acid, a similar increase in the nonanal yield might also be predicted by the mechanism, but neither group was able to detect the volatile product. Using the coated-wall flow tube technique, Thornberry and Abbatt[37] and Moise and Rudich[28] have measured the nonanal yield to be 0.50 and 0.28, respectively, indicating that little nonanal results from such a reaction if it occurs at all. Finally, the small yield of 9-oxooctadecanoic acid ($\sim$0.02) measured in the current work leads us to conclude that while the Martin mechanism may exist as a minor pathway, it is not sufficient to explain our observed yields.

5. Summary and Conclusions

The uptake coefficients for the ozonolysis of particles of unsaturated organics indicate an enhanced rate of reaction compared to analogous gas-phase reactions and agree well with previous measurements. Five products are identified from the reaction of O_3 with oleic acid particles, and all five are found on the reacted particles, though nonanal partially evaporates. The sizable fraction of nonanal that remains on the particles may indicate that aged particles effectively lower the vapor pressures of such volatile or semi-volatile species, and further work is required to assess the magnitude of this effect. Finally, the relative yields of the products within each reaction pathway are found to be unequal, suggesting that the Criegee intermediates react with one another to form additional nonanal and 9-oxononanoic acid. These reactions may only occur in the presence of high O_3 concentrations, such as used in these laboratory experiments, and further study is required to determine their significance under typical tropospheric conditions.

Acknowledgment. We gratefully acknowledge support from the American Chemical Society Petroleum Research Fund and the University of Georgia Research Foundation. We also thank Amanda Lovett for assistance with aerosol generation.

References and Notes

(1) Ketseridis, G.; Hahn, J.; Jaenicke, R.; Junge, C. *Atmos. Environ.* **1976**, *10*, 603−610.
(2) Rogge, W. F.; Hildemann, L. M.; Mazurek, M. A.; Cass, G. R.; Simoneit, B. R. T. *Environ. Sci. Technol.* **1991**, *25*, 1112−1125.
(3) Simoneit, B. R. T.; Sheng, G.; Chen, X.; Fu, J.; Zhang, J.; Xu, Y. *Atmos. Environ. A* **1991**, *25A*, 2111−2129.
(4) Rogge, W. F.; Hildemann, L. M.; Mazurek, M. A.; Cass, G. R.; Simoneit, B. R. T. *Environ. Sci. Technol.* **1993**, *27*, 636−651.
(5) Matsumoto, K.; Tanaka, H.; Nagao, I.; Ishizaka, Y. *Geophys. Res. Lett.* **1997**, *24*, 655−658.
(6) Novakov, T.; Corrigan, C. E.; Penner, J. E.; Chuang, C. C.; Rosaria, O.; Mayol Bracero, O. L. *J. Geophys. Res.* **1997**, *102*, 21307−21313.
(7) Murphy, D. M.; Thomson, D. S.; Mahoney, M. J. *Science* **1998**, *282*, 1664−1669.
(8) Middlebrook, A. M.; Murphy, D. M.; Thomson, D. S. *J. Geophys. Res.* **1998**, *103*, 16475−16483.
(9) Schauer, J. J.; Kleeman, M. J.; Cass, G. R.; Simoneit, B. R. T. *Environ. Sci. Technol.* **1999**, *33*, 1578−1587.
(10) Kavouras, I. G.; Stephanou, E. G. *J. Geophys. Res.* **2002**, *107*, AAC 7/1−AAC 7/13.
(11) Simoneit, B. R. T. *J. Atmos. Chem.* **1989**, *8*, 251−275.
(12) Finlayson-Pitts, B. J.; Pitts, J. J. N. *Chemistry of the Upper and Lower Atmosphere: Theory, Experiments, and Applications*; Academic Press: San Diego, CA, 2000.
(13) Gill, P. S.; Graedel, T. E.; Weschler, C. J. *Rev. Geophys. Space Phys.* **1983**, *21*, 903−920.
(14) Ellison, G. B.; Tuck, A. F.; Vaida, V. *J. Geophys. Res.* **1999**, *104*, 11633−11641.
(15) Facchini, M. C.; Mircea, M.; Fuzzi, S.; Charlson, R. J. *Nature* **1999**, *401*, 257−259.
(16) Tervahattu, H.; Juhanoja, J.; Kupiainen, K. *J. Geophys. Res.* **2002**, *107*, ACH18/11-ACH18/17.
(17) Tervahattu, H.; Hartonen, K.; Kerminen, V.-M.; Kupiainen, K.; Aarnio, P.; Koskentalo, T.; Tuck, A. F.; Vaida, V. *J. Geophys. Res.* **2002**, *107*, AAC 1/1−AAC 1/9.
(18) Mochida, M.; Kitamori, Y.; Kawamura, K.; Nojiri, Y.; Suzuki, K. *J. Geophys. Res.* **2002**, *107*, AAC1/1−AAC1/10.
(19) Russell, L. M.; Maria, S. F.; Myneni, S. C. B. *Geophys. Res. Lett.* **2002**, *29*, 26/21−26/24.
(20) Saxena, P.; Hildemann, L. M.; McMurry, P. H.; Seinfeld, J. H. *J. Geophys. Res.* **1995**, *100*, 18/755−718/770.
(21) Rudich, Y. *Chem. Rev.* **2003**, *103*, 5097−5124.
(22) Cooper, P.; Abbatt, J. P. D. *J. Phys. Chem.* **1996**, *100*, 2249−2254.
(23) De Gouw, J. A.; Lovejoy, E. R. *Geophys. Res. Lett.* **1998**, *25*, 931−934.

(24) Tobias, H. J.; Ziemann, P. J. *Anal. Chem.* **1999**, *71*, 3428−3435.
(25) Wadia, Y.; Tobias, D. J.; Stafford, R.; Finlayson-Pitts, B. J. *Langmuir* **2000**, *16*, 9321−9330.
(26) Thomas, E. R.; Frost, G. J.; Rudich, Y. *J. Geophys. Res.* **2001**, *106*, 3045−3056.
(27) Bertram, A. K.; Ivanov, A. V.; Hunter, M.; Molina, L. T.; Molina, M. J. *J. Phys. Chem. A* **2001**, *105*, 9415−9421.
(28) Moise, T.; Rudich, Y. *J. Phys. Chem. A* **2002**, *106*, 6469−6476.
(29) Morris, J. W.; Davidovits, P.; Jayne, J. T.; Jimenez, J. L.; Shi, Q.; Kolb, C. E.; Worsnop, D. R.; Barney, W. S.; Cass, G. *Geophys. Res. Lett.* **2002**, *29*, 71/71−71/74.
(30) Smith, G. D.; Woods, E., III; DeForest, C. L.; Baer, T.; Miller, R. E. *J. Phys. Chem. A* **2002**, *106*, 8085−8095.
(31) Michel, A. E.; Usher, C. R.; Grassian, V. H. *Geophys. Res. Lett.* **2002**, *29*, 10/11−10/14.
(32) Esteve, W.; Budzinski, H.; Villenave, E. *Polycyclic Aromat. Compd.* **2003**, *23*, 441−456.
(33) Mmereki, B. T.; Donaldson, D. J. *J. Phys. Chem. A* **2003**, *107*, 11038−11042.
(34) Eliason, T. L.; Aloisio, S.; Donaldson, D. J.; Cziczo, D. J.; Vaida, V. *Atmos. Environ.* **2003**, *37*, 2207−2219.
(35) Eliason, T. L.; Gilman, J. B.; Vaida, V. *Atmos. Environ.* **2004**, *38*, 1367−1378.
(36) Katrib, Y.; Martin, S.; Hung, H.-M.; Rudich, Y.; Zhang, H.; Slowik, J.; Davidovits, P.; Jayne, J. T.; Worsnop, D. R. *J. Phys. Chem. A* **2004**, *108*, 6686−6695.
(37) Thornberry, T. D.; Abbatt, J. P. D. *Phys. Chem. Chem. Phys.* **2004**, *6*, 84−93.
(38) LaFranchi, B.; Zahardis, J.; Petrucci, G. *Proceedings of the 52nd Conference of the American Society for Mass Spectrometry*; Nashville, TN, May, 2004.
(39) Limbeck, A.; Puxbaum, H. *Atmos. Environ.* **1999**, *33*, 1847−1852.
(40) Srisankar, E. V.; Patterson, L. K. *Arch. Environ. Health* **1979**, *34*, 346−349.
(41) Schwartz, S. E.; Freiberg, J. E. *Atmos. Environ.* **1981**, *15*, 1129−1144.
(42) Kolb, C. E.; Zahniser, M.; Davidovits, P.; Keyser; Leu; Molina, M. J.; Hanson, D. R.; Ravishankara, A. R. In *Progress and Problems in Atmospheric Chemistry*. [In *Adv. Ser. Phys. Chem.*; 1995; 3]; Barker, J. R., Ed., 1995.
(43) Hanson, D. R. *J. Phys. Chem. B* **1997**, *101*, 4998−5001.
(44) Worsnop, D. R.; Morris, J. W.; Shi, Q.; Davidovits, P.; Kolb, C. E. *Geophys. Res. Lett.* **2002**, *29*, 57/51−57/54.
(45) Hearn, J. D.; Smith, G. D. *Anal. Chem.* **2004**, *76*, 2820−2826.
(46) Razumovskii, S. D.; Zaikov, G. E. *Zh. Org. Khim.* **1972**, *8*, 468−472.
(47) Hanson, D. R.; Ravishankara, A. R.; Solomon, S. *J. Geophys. Res.* **1994**, *99*, 3615−3629.
(48) Bailey, P. S. *Ozonation in Organic Chemistry*; Academic Press: New York, 1978; Vol. 1.
(49) Criegee, R. *Angew. Chem. Int. Ed.* **1975**, *14*, 745−752.
(50) Daubert, T. E.; Danner, R. P. *Physical and Thermodynamic Properties of Pure Chemicals: Data Compilation*; Hemisphere: New York, 1989.
(51) Verevkin, S. P.; Krasnykh, E. L.; Vasiltsova, T. V.; Koutek, B.; Doubsky, J.; Heintz, A. *Fluid Phase Equilib.* **2003**, *206*, 331−339.
(52) Moise, T.; Rudich, Y. *Geophys. Res. Lett.* **2001**, *28*, 4083−4086.
(53) Vieceli, J.; Ma, O. L.; Tobias, D. J. *J. Phys. Chem. A* **2004**, *108*, 5806−5814.
(54) Smith, G. D.; Woods, E., III; Baer, T.; Miller, R. E. *J. Phys. Chem. A* **2003**, *107*, 9582−9587.
(55) Rebrovic, L. *J. Am. Oil Chem. Soc.* **1992**, *69*, 159−165.
(56) Fliszar, S.; Gravel, D.; Cavalieri, E. *Can. J. Chem.* **1966**, *44*, 1013−1019.
(57) Fliszar, S.; Chylinska, J. B. *Can. J. Chem.* **1968**, *46*, 783−788.